DOI: 10.1002/ejic.200901210

An Oximate-Free Ferromagnetically Coupled Triangular $[Mn^{III}_3(\mu_3\text{-}O)]^{7+}$ Core

Phalguni Chaudhuri,*[a] Rita Wagner,[a] and Thomas Weyhermüller[a]

Keywords: Manganese / Schiff bases / Magnetic properties / Ferromagnetism

The Schiff-base ligand H_2L, *N*-(2-hydroxymethylphenyl)salicylideneimine yields a trimanganese(III) complex, $[L_3Mn^{III}_3(\mu_3\text{-}O)(MeOH)_3]PF_6$ (**1**), in which monoatomic alkoxo-bridging is present along the edges of the Mn_3-triangle containing d^4 high-spin manganese(III) centers, which are ferromagnetically coupled resulting in an $S_t = 6$ spin ground state for **1**.

Introduction

The triangular $[Mn_3(\mu_3\text{-}O)]^{7+}$ core is found very often in the chemistry of manganese(III). A very well-known example is the trinuclear carboxylates of general formula $[Mn^{III}_3(\mu_3\text{-}O)(\mu\text{-}CO_2R)_6L_3]^+$ in which L represents a monodentate ligand like H_2O, pyridine, acetonitrile, etc. and these so-called "basic carboxylates" exhibit antiferromagnetic exchange interactions within the $[Mn^{III}_3O]$ core.[1] Only recently oximate-bridging has been found to induce structural distortion in the $[Mn_3O]$ core, which yielded in some cases ferromagnetic exchange coupling leading to a resultant ($S_{Mn} = 2$) $S_t = 6$ spin ground state.[2] Although the first ferromagnetic triangular Mn^{III}_3 was found in $[Mn_3O(bamen)_3]^+$ complex cation,[3] where H_2bamen represents the hexadentate oxime ligand 1,2-bis(biacetylmonoximeimino)ethane, the second example $[Mn_3O(mpko)_3(O_2CMe)_3]^+$ (Hmpko = methyl 2-pyridyl ketone oxime) being the first triangular SMM attracted much attention and was subjected to various physical methods.[4] The fascinating observation of ferromagnetic exchange interactions in the oxime-containing triangular $[Mn^{III}_3\text{-}O]$ complexes has led not only to computational DFT calculations[5] but also to additional examples of $S = 6$ $[Mn_3O]$ triangles with other oximes.[6] Herein we report an oximate-free, and also carboxylate-free, ferromagnetic exchange-coupled $[L_3Mn^{III}_3O(CH_3OH)_3]PF_6$ complex (**1**), in which H_2L is an unsymmetrical dibasic ligand, *N*-(2-hydroxymethylphenyl)salicylideneimine, containing both phenol and alcohol OH groups derived from salicylaldehyde and 2-aminobenzyl alcohol. A very similar defect-cubane core $[Mn^{III}_3(\mu_3\text{-}O)\text{-}(\mu\text{-}OR)_3]^{4+}$ with the ligand H_2L', 2-(5-bromosalicylideneamino)-1-propanol (complex **2**), in which the manganese(III) centers in contrast to complex **1** are antiferromagnetically coupled, has been reported.[7]

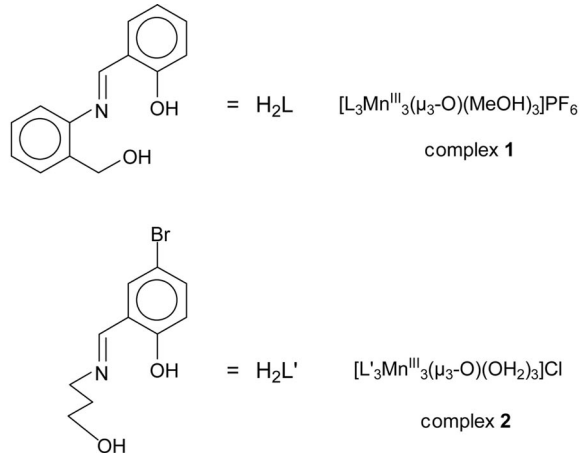

Results and Discussion

The reaction of $MnCl_2{\cdot}4H_2O$ with the ligand H_2L and Et_3N in methanol in the presence of air yields the trinuclear cation $[L_3Mn^{III}_3(\mu_3\text{-}O)(MeOH)_3]^+$ which was isolated as dark red-brown crystals with PF_6^- as anions. In absence of the PF_6-anions, the corresponding chloride salt could also be isolated and was also structurally characterized. In the ESI-positive mass spectrum of **1** a peak with an abundance of 100% is observed centered around $m/z = 856$, corresponding to $[Mn_3L_3O]^+$.

The complex cation of **1** is depicted in Figure 1 and selected interatomic distances and angles are listed in Table 1. The monocation involves three dianionic ligand (L^{2-}), one μ_3-oxo group, three neutral methanol molecules (partially substituted by H_2O), and three manganese ions. Thus, all the manganese ions are in the +III oxidation state, which is also in conform with the observed Mn–O and Mn–N bond lengths. Additionally, the Mn atoms exhibit Jahn–Teller distortions as expected for high-spin d^4 ions in an octahedral geometry. The cation of **1** consists of the core comprising a $[Mn^{III}_3O]^{7+}$ triangular unit with three alkoxide oxygens, O(17), O(37), and O(57) bridging between adjacent Mn^{III} centers.

[a] Max-Planck-Institute for Bioinorganic Chemistry,
Stiftstrasse 34–36, 45470 Mülheim an der Ruhr, Germany
Fax: +49-208-306-3951
E-mail: chaudh@mpi-muelheim.mpg.de

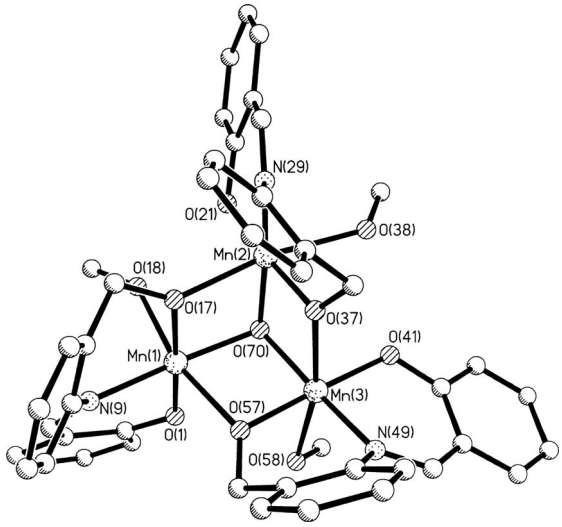

Figure 1. Molecular structure of the cation in **1**.

The coordination environment around the trivalent manganese ions is $MnNO_5$, a distorted octahedron, with an alkoxo oxygen O(17), an azomethine nitrogen N(9) and a phenolate oxygen O(1) from a deprotonated ligand L^{2-}, a second alkoxo-bridging O(57) from the neighboring L^{2-} and a methanol oxygen O(18) donor atom for Mn(1).

The Jahn–Teller (JT) axial elongations are observed along the O(18)–Mn(1)–O(57), O(38)–Mn(2)–O(17) and O(58)–Mn(3)–O(37) axes, thus avoiding the Mn^{III}–O^{2-}(70) bond for the JT elongation, as expected. The JT axes of the Mn^{III} ions are not parallel to each other. The Mn to central oxygen atom, μ_3-O(70), distances at 1.932(2), 1.927(2), 1.936(2) are comparable with those reported for trinuclear [$Mn^{III}_3(\mu_3$-O)] units. The central oxygen atom O(70) is displaced by 0.824 Å from the Mn^{III}_3 plane. The three manganese atoms are at the apices of an isosceles triangle, as is shown by the Mn(1)···Mn(2), Mn(2)···Mn(3), and Mn(3)···Mn(1) distances at 3.003(1) Å, 2.995(1) Å and 3.023(1) Å, respectively.

Magnetic susceptibility data for a polycrystalline sample of complex **1** were collected in the temperature range 2–290 K in an applied magnetic field of 1 T to be in the linear range. The magnetic moment μ_{eff} for **1** of 9.034 μ_B ($\chi_M \cdot T$ = 10.205 $cm^3 mol^{-1} K$) at 290 K increases monotonically with decreasing temperature until it reaches a plateau with a value of 12.226 μ_B ($\chi_M T$ = 18.690 $cm^3 mol^{-1} K$) at about 15 K which is not far from the "spin-only" value of μ_{eff} = 12.96 μ_B for an S = 6 (Figure 2). Below 15 K, μ_{eff} drops to 8.934 μ_B at 2 K due to the combined effects of field saturation, exchange and single-ion zero-field splitting. This temperature-dependence is in agreement with a moderate ferromagnetic coupling between the neighboring Mn^{III} ions with S_{Mn} = 2, resulting in an S_t = 6 ground state for **1**.

To determine the individual pairwise exchange parameters prevailing between the paramagnetic manganese(III) (S_{Mn} = 2.0) pairs in **1**, the susceptibility data were simulated based on the Heisenberg spin Hamiltonian in the form $H = -2J \vec{S}_i \cdot \vec{S}_j$ for a trinuclear complex, using a least-squares

Table 1. Selected bond lengths [Å] and angles [°] for the cation in complex **1**.

Mn(1)···Mn(2)	3.0034(6)	O(17)–Mn(1)–O(1)	174.83(10)
Mn(1)···Mn(3)	3.0233(6)	O(17)–Mn(1)–O(70)	84.14(7)
Mn(2)···Mn(3)	2.9950(6)	O(1)–Mn(1)–O(70)	95.60(8)
Mn(1)–O(17)	1.8767(17)	O(17)–Mn(1)–N(9)	91.11(8)
Mn(1)–O(1)	1.8950(19)	O(1)–Mn(1)–N(9)	89.78(8)
Mn(1)–O(70)	1.9320(17)	O(70)–Mn(1)–N(9)	171.29(8)
Mn(1)–N(9)	2.022(2)	O(17)–Mn(1)–O(57)	93.14(8)
Mn(1)–O(57)	2.219(2)	O(1)–Mn(1)–O(57)	91.82(10)
Mn(1)–O(18)	2.256(5)	O(70)–Mn(1)–O(57)	76.58(7)
Mn(2)–O(37)	1.8738(17)	N(9)–Mn(1)–O(57)	96.45(8)
Mn(2)–O(21)	1.8975(17)	O(17)–Mn(1)–O(18)	85.1(2)
Mn(2)–O(70)	1.9265(16)	O(1)–Mn(1)–O(18)	89.7(2)
Mn(2)–N(29)	2.0144(19)	O(70)–Mn(1)–O(18)	89.14(19)
Mn(2)–O(17)	2.1602(17)	N(9)–Mn(1)–O(18)	97.8(2)
Mn(2)–O(38)	2.3350(18)	O(57)–Mn(1)–O(18)	165.72(19)
Mn(3)–O(57)	1.871(2)	O(37)–Mn(2)–O(21)	173.61(8)
Mn(3)–O(41)	1.9074(18)	O(37)–Mn(2)–O(70)	84.78(7)
Mn(3)–O(70)	1.9359(17)	O(21)–Mn(2)–O(70)	93.69(7)
Mn(3)–N(49)	2.026(2)	O(37)–Mn(2)–N(29)	91.56(8)
Mn(3)–O(37)	2.1601(17)	O(21)–Mn(2)–N(29)	90.77(8)
Mn(3)–O(58)	2.257(3)	O(70)–Mn(2)–N(29)	171.44(8)
		O(37)–Mn(2)–O(17)	91.85(7)
Mn(2)–O(70)–Mn(1)	102.23(8)	O(21)–Mn(2)–O(17)	93.86(8)
Mn(2)–O(70)–Mn(3)	101.69(7)	O(70)–Mn(2)–O(17)	77.07(7)
Mn(1)–O(70)–Mn(3)	102.82(8)	N(29)–Mn(2)–O(17)	95.36(7)
Mn(1)–O(17)–Mn(2)	95.89(7)	O(37)–Mn(2)–O(38)	82.55(7)
Mn(2)–O(37)–Mn(3)	95.62(7)	O(21)–Mn(2)–O(38)	91.35(7)
Mn(3)–O(57)–Mn(1)	94.95(9)	O(70)–Mn(2)–O(38)	93.12(7)
		N(29)–Mn(2)–O(38)	94.07(7)
		O(17)–Mn(2)–O(38)	169.15(7)
		O(57)–Mn(3)–O(41)	175.08(9)
		O(57)–Mn(3)–O(70)	85.41(8)
		O(41)–Mn(3)–O(70)	94.09(7)
		O(57)–Mn(3)–N(49)	91.64(9)
		O(41)–Mn(3)–N(49)	89.64(8)
		O(70)–Mn(3)–N(49)	170.17(8)
		O(57)–Mn(3)–O(37)	94.11(9)
		O(41)–Mn(3)–O(37)	90.55(7)
		O(70)–Mn(3)–O(37)	77.23(7)
		N(49)–Mn(3)–O(37)	93.66(8)
		O(57)–Mn(3)–O(58)	78.82(12)
		O(41)–Mn(3)–O(58)	96.32(11)
		O(70)–Mn(3)–O(58)	92.29(12)
		N(49)–Mn(3)–O(58)	96.34(12)
		O(37)–Mn(3)–O(58)	167.88(11)

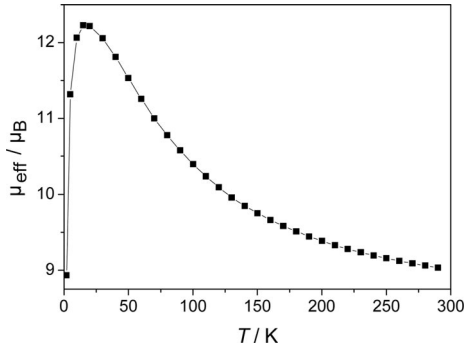

Figure 2. A plot of the experimental effective magnetic moment M, μ_{eff} (squares) for complex **1** as a function of temperature (T). The solid line represents the best fit with the full-diagonalization matrix method using the parameters given in the text.

fitting computer program[8] with a full-matrix diagonalization method. Fits of the data to a one-J model for a C_3 equilateral triangle gave very poor fits. As even crystallographically equilateral [Mn_3O] triangles are known to undergo the magnetic Jahn–Teller distortion, resulting in an isosceles situation, we have used an isosceles triangle model (two-J, C_{2v} symmetry) for simulation. The Mn···Mn distances in **1** are also in accord with this model. Thus, two exchange parameters J and J' referring to the $Mn^{III}Mn^{III}$ (S_{Mn} = 2.0) exchange interactions were required to simulate the experimental data, shown as the solid line in the plot of μ_{eff} vs. T (Figure 2). The best fit parameters obtained are J = +10.0 cm^{-1}, J' = +3.2 cm^{-1}, g_{Mn} = 1.915, D = –0.3 cm^{-1}. No other parameters had to be invoked to obtain the simulation shown as the solid line in Figure 2.

The properties of the ground-state spin manifolds were further probed by variable-temperature variable-field (VTVH) measurements at 1, 4 and 7 T, with data sets sampled on a 1/T scale in the range 2–260 K; we have collected most of the magnetization data in the temperature range 2.0–15 K (29 data points) and only 4 data points in the range 15–260 K, which are shown in Figure 3 as plots of $M/Ng\mu B$ vs. $\mu_b B/kT$. The data sets at different magnetic fields are nearly super imposable, particularly data for 4 and 7 T, indicating the presence of small zero-field splitting (D_{Mn}) in the ground state. From Figure 3 it is clear that the magnetization value tends to a saturation value of ca. 5.96 which agrees well with the S_t = 6.0 ground state for **1**. The solid line shown in Figure 3 was simulated with the parameters J = +10.0 cm^{-1}, J' = +3.2 cm^{-1}, g_{Mn} = 1.98, and D = –0.3 cm^{-1}, which agree well with the 1 T-measurement (Figure 2).

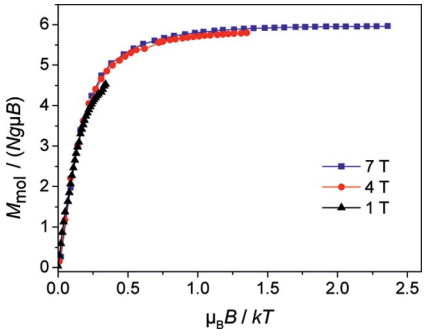

Figure 3. A plot of VTVH measurements for complex **1**. The solid lines represent the best fit parameters given in the text.

Based on the nature of the bridging atoms and exchange integrals the [$Mn^{III}_3(\mu_3\text{-}O)$]$^{7+}$ units including complexes **1** and **2** can be divided into five groups:

Group 1: The ubiquitious "basic carboxylates" containing only triatomic carboxylate bridges, in which the μ_3-O^{2-} ion lies in the Mn_3 plane, exhibit antiferromagnetic exchange interactions.[1]

Group 2: A single example of ferromagnetically coupled[3] Mn^{III} centers bridged by only diatomic oximate bridges; the μ_3-O^{2-} is not displaced from the Mn_3 plane.

Group 3: There are many examples,[2,4] of mixed oximate and carboxylate bridges with the μ_3-O^{2-} ion displaced (≈ 0.3 Å) from the Mn_3 plane; the nature of exchange interactions reported varies from antiferromagnetism to ferromagnetism.

Group 4: The trinuclear manganese(III) complex is based on an asymmetric oximate-bridged [$Mn^{III}_3(\mu_3\text{-}O)(\mu_2\text{-}OPh)$]$^{6+}$ core[9] which can be viewed as a trinuclear [Mn_3O]$^{7+}$ unit to which has been added an phenoxide PhO^- moiety. For the manganese(III) compound, the antiferromagnetic contributions are balanced by the ferromagnetic contributions resulting in three manganese(III) centers being practically uncoupled.

Group 5: There are two examples of monoatomic alkoxo-bridged compounds with the central μ_3-O^{2-} ion ca. 0.8 Å above the Mn_3 plane. Complex **1** described in this paper shows ferromagnetic coupling, whereas complex **2**[7] with nearly identical structural parameters, e.g. the Mn–μ_3-O–Mn angles, the Mn–μ_2-O(alkoxide)–Mn angles, the Mn–N and Mn–O distances, contains Mn^{III} centers which on the contrary are antiferromagnetically coupled. Thus, displacement of the μ_3-O^{2-} ion from the Mn_3 plane cannot be the key factor for the origin of ferromagnetism in the [Mn_3O]$^{7+}$ triangles. During the progress of this communication, the third monoatomic alkoxo-bridged compound, complex **3**, with the ligand 2,6-bis(hydroxymethyl)-*p*-cresol (H_3hmc) is reported.[10] The anion of **3** contains a ferromagnetically coupled [$Mn^{III}_3(\mu_3\text{-}O)$]$^{7+}$ triangular core, with the central μ_3-O^{2-} ion lying 0.765 Å above the Mn_3 plane. The strength of exchange interactions (J = +8.7 cm^{-1}, J' = +1.2 cm^{-1}) for **3** is weaker, the difference being small but significant, than that in **1** and thus in conform with the argument of displacement of the O^{2-} ion from the Mn_3 plane as the sole cause of ferromagnetism. In this connection, some subtle differences between complexes **1** and **3** are noteworthy. The three Mn–μ_3-O distances in **1** are nearly identical at ca. 1.93 Å, whereas there are two distinctly different Mn–μ_3-O distances in **3** with ca. 2.00 and ca. 1.86 Å. Additionally, the Mn–μ_2-O(alkoxide)–Mn angles differ appreciably in the complexes **1** and **3**.

Recently DFT calculations[5] have been performed in an attempt to rationalize the observed change from S = 6 to S = 2 for Group 3 molecules; the non-parallel alignment of the JT axes is suggested to be an important factor for the ferromagnetic properties of the oximate-bridged molecules. Indeed, the JT axes are non-parallel in complex **1** without an oximate-bridge exhibiting an S = 6 ground state. Unfortunately, the magnetic behavior of complex **2** with S = 2 ground state cannot be explained on the basis of alignment of JT axes, which are also non-parallel in **2**.

Triangular [$Mn^{III}_3(\mu_3\text{-}O)$]$^{7+}$ units are thus of great relevance for better understanding of the magnetic behavior of these simple trinuclear complexes, as they would result in rationalization of the physical properties of more complex structures based on these triangles.

Experimental Section

H_2L: The ligand *N*-[2-(hydroxymethyl)phenyl]salicylideneimine was prepared as described previously[11] by refluxing a solution of 2-

aminobenzyl alcohol (6.15 g; 50 mmol) and salicylaldehyde (6.1 g; 50 mmol) in distilled ethanol (70 mL) for 1 h which resulted in a yellow microcrystalline solid after concentration. The yellow solid was collected by filtration, washed with *n*-pentane and air-dried; yield 10.5 g (≈ 92%); m.p. 118–119 °C. EI-MS: *m*/*z* (%) = 227 (66) $[M]^+$, 209 (69) $[M - OH_2]^+$, 180 (58) $[M - CH_4O_2]^+$, 121 (18.6) $[M - C_7H_7O]^+$, 106 (100) $[M - C_7H_7NO]^+$. ^1H NMR (250 MHz, in $CDCl_3$): δ = 8.59 (s, 1 H), 7.48–7.49 (d, 1 H), 7.33–7.42 (m, 4 H), 7.12–7.15 (m, 1 H), 6.91–7.04 (m, 2 H), 4.86 (s, 2 H) ppm. Selected IR data (KBr): $\tilde{\nu}$ = 3400, 3280, 1617, 1565, 1482, 1454, 1279, 1179, 1150, 1031, 909, 820, 760, 706 cm^{-1}.

Purity of the ligand was checked by gas chromatography to be >99%, instrument HP 6890, detector FID, temp. 80–400 °C (8 °C/min), column: 2B-5HT (0.1 μm), run time 48 min.

$[L_3Mn_3(\mu_3\text{-}O)(CH_3OH)_{2.35}(OH_2)_{0.65}]PF_6 \cdot 0.39H_2O$ (1): To a solution of H_2L (0.23 g; 1 mmol) in methanol (50 mL) was added solid $MnCl_2 \cdot 4H_2O$ (0.2 g; 1 mmol) with stirring, followed by the addition of Et_3N (0.5 mL; 3.6 mmol). The resulting brown solution was refluxed for 0.5 h, stirred for further 1 h in air after addition of solid *n*-tetrabutylammonium hexafluorophosphate (0.13 g) and filtered to remove any solid particles. The yellow-brown solution was allowed to concentrate slowly at room temperature to yield X-ray quality crystals of **1**, which were separated by filtration; yield 500 mg (≈ 46%). $C_{44.35}H_{44.48}F_6Mn_3N_3O_{10.39}P$ (1095.5): calcd. C 48.62, H 4.09, N 3.84, Mn 15.04; found C 48.1, H 4.1, N 3.9, Mn 16.2. IR (KBr): $\tilde{\nu}$ = 3643, 3556, 3379, 1607, 1578, 1535, 1466, 1435, 1381, 1302, 1227, 1181, 1151, 1128, 1112, 1057, 1041, 988, 927, 879, 842, 782, 758, 654, 628, 607, 558 cm^{-1}. MS-ESI positive (MeOH): *m*/*z* (%) = 856.1 $[Mn_3L_3O]^+$, 577.1 $[Mn_2L_2O]^+$. UV/Vis in MeOH: (λ_{max}) [ε $M^{-1}cm^{-1}$]: 407 (17700), 238 (73800).

X-ray Crystallographic Data Collection and Refinement of the Structure: Formula: $C_{44.35}H_{44.48}F_6Mn_3N_3O_{10.39}P$, fw = 1095.52, T = 100(2) K, triclinic, space group $P\bar{1}$ (No. 2), a = 14.0718(14) Å, b = 14.1770(14) Å, c = 14.7220(15) Å, α = 67.643(2)°, β = 83.254(2)°, γ = 60.845(2)°, V = 2363.7(4) $Å^3$, Z = 2, ρ(calcd.) = 1.539 $g\,cm^{-3}$, unique reflections [$I > 2\sigma(I)$] 17077(12495), No. of parameters 779, R_1 = 0.0535, wR_2 = 0.1405, goodness-of-fit on F^2 = 1.033.

A dark brown single crystal of **1**·0.39H_2O was coated with perfluoropolyether, picked up with nylon loops and was immediately mounted in the nitrogen cold stream of the diffractometers to prevent the loss of solvent. A Bruker APEX II diffractometer was utilized for **1**·0.39H_2O to collect intensity data. A Mo-target rotating-anode X-ray source (Mo-K_α radiation, λ = 0.71073 Å) and a graphite monochromator was used throughout. Final cell constants were obtained from least-squares fits of several thousand strong reflections. Intensity data were corrected for absorption using intensities of redundant reflections with the program SADABS.[12] The structure was readily solved by Patterson methods and subsequent difference Fourier techniques. The Siemens ShelXTL[13] software package was used for solution and artwork of the structure, ShelXL97[14] was used for the refinement. All non-hydrogen atoms were anisotropically refined and hydrogen atoms bound to carbon were placed at calculated positions and refined as riding atoms with isotropic displacement parameters. Hydrogen atoms bound to oxygen atoms in coordinated and uncoordinated methanol and water molecules in **1** could not be reliably localized.

The structure refinement of **1**·0.39H_2O turned out to be very difficult though crystal and data quality were found to be good. The PF_6^- anion of the complex resides on two special positions, namely inversion centers, of which one position is extremely disordered (at 0, 0.5, 0). This is due to a mixing of methanol and water molecules bound to the sixth coordination site of the manganese(III) ions. Coordination sites at Mn(1) and Mn(3) are much more affected than Mn(2). Different space requirements and formation of hydrogen bonds of coordinated water/methanol molecules to the aforementioned PF_6^- anion lead to the observed disorder. Several disorder models having the central phosphorus atom on and off the inversion center were tried but none of them was completely satisfying. Finally, a rigid body refinement of three disordered positions off the inversion center was chosen and solvent molecules at Mn(1) and Mn(3) were allowed to mix. The MeOH/H_2O occupation ratio at Mn(1) refined to about 0.74:0.26 and at Mn(3) to a ratio of about 0.61:0.39.

CCDC-758037 contains the supplementary crystallographic data for this paper. These data can be obtained free of charge from the Cambridge Crystallographic Data Centre via www.ccdc.cam.ac.uk/data_request/cif.

Acknowledgments

This work was supported by the Deutsche Forschungsgemeinschaft (DFG) (Priority Program: "Molecular Magnetism", Ch111/3-3). Thanks are due to H. Schucht and A. Goebels for their skilful technical assistance.

[1] a) R. D. Cannon, R. P. White, *Prog. Inorg. Chem.* **1988**, *36*, 195; b) R. D. Cannon, U. A. Jayasooriya, R. Wu, S. K. Arapkoske, J. A. Stride, O. F. Nielsen, R. P. White, G. J. Kearley, D. J. Summerfields, *J. Am. Chem. Soc.* **1994**, *116*, 11869.
[2] R. Inglis, S. M. Taylor, L. F. Jones, G. S. Papaefstathiou, S. P. Perlepes, S. Datta, S. Hill, W. Wernsdorfer, E. K. Brechin, *Dalton Trans.* **2009**, 9157.
[3] S. G. Sreerama, S. Pal, *Inorg. Chem.* **2002**, *41*, 4843.
[4] a) T. C. Stamatos, D. Foguet-Albiol, C. C. Stoumpos, C. P. Raptopoulou, A. Terzis, W. Wernsdorfer, S. P. Perlepes, G. Christou, *J. Am. Chem. Soc.* **2005**, *127*, 15380; b) T. C. Stamatos, D. Foguet-Albiol, S.-C. Lee, C. C. Stoumpos, C. P. Raptopoulou, A. Terzis, W. Wernsdorfer, S. O. Hill, S. P. Perlepes, G. Christou, *J. Am. Chem. Soc.* **2007**, *129*, 9484.
[5] J. Cano, T. Cauchy, E. Ruiz, C. J. Milios, C. C. Stoumpos, T. C. Stamatos, S. P. Perlepes, G. Christou, E. K. Brechin, *Dalton Trans.* **2008**, 234.
[6] C.-I. Yang, W. Wernsdorfer, K.-H. Cheng, M. Nakano, G.-H. Lee, H.-L. Tsai, *Inorg. Chem.* **2008**, *47*, 10184.
[7] M. Nihei, N. Hoshino, T. Ito, H. Oshio, *Chem. Lett.* **2002**, 1016.
[8] E. Bill, Max-Planck-Institut für Bioanorganische Chemie, Mülheim an der Ruhr, Germany, **2005**.
[9] P. Chaudhuri, *Coord. Chem. Rev.* **2003**, *243*, 159.
[10] C. Lampropoulos, K. A. Abbond, T. C. Stamatatos, G. Christou, *Inorg. Chem.* **2009**, *48*, 813.
[11] a) A. Syamal, K. S. Kale, *Indian J. Chem., Ser. A* **1980**, *19*, 225; b) A. Syamal, K. S. Kale, *Indian J. Chem., Ser. A* **1980**, *19*, 488; c) B. Jezowska-Trzebiatowska, J. Lisowski, A. Vogt, P. Chmielewski, *Polyhedron* **1988**, *7*, 337; d) M. Koikawa, H. Yamashita, T. Tokii, *Inorg. Chim. Acta* **2004**, *357*, 2635; e) M. Koikawa, K. Iwashita, T. Tokii, *Acta Crystallogr., Sect. E* **2004**, *60*, m239; f) M. Koikawa, M. Ohba, T. Tokii, *Polyhedron* **2005**, *24*, 2257.
[12] *SADABS*, Bruker-Siemens Area Detector Absorption and Other Correction, G. M. Sheldrick, University of Göttingen, Germany, **2006**, version 2006/1.
[13] *ShelXTL* v. 6.14, Bruker AXS Inc., Madison, WI, USA **2003**.
[14] *ShelXL97*, G. M. Sheldrick, University of Göttingen, Germany, **1997**.

Received: December 15, 2009
Published Online: February 19, 2010

